

QUANTAL EFFECTS ON SPINODAL INSTABILITIES IN CHARGE ASYMMETRIC NUCLEAR MATTER

S. Ayik^{1,*}, N. Er², O. Yilmaz², and A. Gokalp²

¹*Physics Department, Tennessee Technological University, Cookeville, TN 38505, USA*

²*Physics Department, Middle East Technical University, 06531 Ankara, Turkey*

(Dated: October 27, 2018)

Abstract

Quantal effects on growth of spinodal instabilities in charge asymmetric nuclear matter are investigated in the framework of a stochastic mean field approach. Due to quantal effects, in both symmetric and asymmetric matter, dominant unstable modes shift towards longer wavelengths and modes with wave numbers larger than the Fermi momentum are strongly suppressed. As a result of quantum statistical effects, in particular at lower temperatures, magnitude of density fluctuations grows larger than those calculated in semi-classical approximation.

PACS numbers: 21.65.+f; 25.70.Pq; 21.60.Ev

*Electronic address: ayik@tntech.edu

I. INTRODUCTION

In many processes, such as induced fission, heavy-ion fusion near barrier energies and spinodal instabilities and nuclear multi-fragmentation, dynamics of density fluctuations play a dominant role. For description of these processes mean-field transport models, such as time-dependent Hartree-Fock (TDHF) [1, 2] and the Boltzmann-Uhling-Uhlenbeck (BUU) [3] models are not very useful. TDHF includes, the so called, one-body dissipation mechanism, but associated fluctuation mechanism is not incorporated into the model. Similarly, the extended TDHF and its semi-classical approximation BUU model involves one-body and collisional dissipation, but the associated fluctuation mechanisms are not included into the description. It is well known that no dissipation takes place without fluctuations. In order to describe dynamics of density fluctuations, we need to develop stochastic transport models by incorporating fluctuation mechanisms into the description. There are two different mechanisms for density fluctuations: (i) collisional fluctuations generated by two-body collisions and (ii) one-body mechanism or mean-field fluctuations. Much effort has been given to improve the transport description by incorporating two-body dissipation and fluctuation mechanisms. The resultant stochastic transport theory, known as Boltzmann-Langevin model [4, 6], provides a suitable framework for dynamics of density fluctuations in nuclear collisions around Fermi energy. However, two-body dissipation and fluctuation mechanisms do not play an important role at low energies. At low bombarding energies, mean-field fluctuations provide the dominant mechanism for fluctuations of collective nuclear motion. In a recent work, we addressed this question [7]. Restricting our treatment at low energies, we proposed a stochastic mean-field approach for nuclear dynamics, which incorporates one-body dissipation and fluctuation mechanisms in accordance with quantum dissipation-fluctuation theorem. Therefore, the stochastic mean-field approach provides a powerful microscopic tool for describing low energy nuclear processes including induced fission, heavy-ion fusion near barrier energies and spinodal decomposition of nuclear matter.

Much work has been done to understand the spinodal instabilities and their connection with liquid gas phase transformation in symmetric and more recently charge asymmetric nuclear matter. Most of these investigations have been carried out in the basis of semi-classical Boltzmann-Langevin (BL) type stochastic transport models [8]. There are two major problems with these investigations. First of all, numerical simulations of BL model are not very

easy, even with approximate methods, simulations require large amount of numerical effort. The second problem is related with the semi-classical description of spinodal decomposition of nuclear matter. According to our previous investigations, quantal statistical effects play an important role in spinodal dynamics [9, 10]. There are qualitatively two different regimes during evolution of nuclear collisions in Fermi energy domain. During the initial regime of heavy ion-collisions, namely, from touching until formation of hot and compressed piece of nuclear matter, collisional dissipation and fluctuations are substantially important. On the other hand, during expansion of the system into mechanically unstable spinodal region, collisional effects may be neglected. In the spinodal region, local density fluctuations, which are accumulated during the initial regime, are mainly driven by the mean-field until system breaks up into clusters. Recently proposed stochastic mean-field approach provides a useful tool for describing spinodal decomposition of expanding hot piece of nuclear matter. The approach includes quantum statistical effects and at the same time, numerical simulations of the approach can be carried out without much difficulty.

In this work, we study early growth of density fluctuations in charge asymmetric nuclear matter and investigate quantum statistical effects on spinodal instabilities and on growth rates of dominant unstable modes on the basis of stochastic mean-field approach. In section 2, we present a brief description of the stochastic mean-field approach. In section 3, we calculate early growth of density fluctuations, growth rates and phase diagram of dominant modes in charge asymmetric systems, and study quantal effects on these quantities. Conclusions are given in section 4.

II. STOCHASTIC MEAN-FIELD APPROACH

In the standard TDHF description of a many-body system, time-dependent wave function is assumed to be a single Slater determinant constructed with time-dependent single-particle wave functions. The standard approach provides a good description for the average evolution of collective motion, however it severely restricts fluctuations of collective motion [1, 2]. In order to describe fluctuations, we must give up single determinantal description and consider superposition of determinantal wave functions. In the stochastic mean-field description, an ensemble of single-particle density matrices associated with the ensemble of Slater determinants is generated in a stochastic framework by retaining only initial correlations [7]. A

member of single-particle density matrix, indicated by label λ , can be expressed as,

$$\rho_a^\lambda(\vec{r}, \vec{r}', t) = \sum_{ij} \Phi_i^*(\vec{r}, t; \lambda) \langle i | \rho_a^\lambda(0) | j \rangle \Phi_j(\vec{r}', t; \lambda). \quad (1)$$

In this expression and in the rest of the paper label $a = n, p$ represents neutron and proton species and $\langle i | \rho_a^\lambda(0) | j \rangle$ are time-independent elements of density matrix determined by the initial correlations. The main assumption of the approach is that each matrix element is a Gaussian random number specified by a mean value $\overline{\langle i | \rho_a^\lambda(0) | j \rangle} = \delta_{ij} \rho_a(i)$ and a variance,

$$\overline{\langle i | \delta \rho_a^\lambda(0) | j \rangle \langle j' | \delta \rho_b^\lambda(0) | i' \rangle} = \frac{1}{2} \delta_{ab} \delta_{ii'} \delta_{jj'} \{ \rho_a(i) [1 - \rho_a(j)] + \rho_a(j) [1 - \rho_a(i)] \}. \quad (2)$$

In these expressions $\langle i | \delta \rho_a^\lambda(0) | j \rangle$ represents fluctuating elements of initial density matrix, $\rho_a(j)$ denotes the average occupation number. At zero temperature, the average occupation numbers are zero and one and at finite temperature, they are given by the Fermi-Dirac distribution. In each event, different from the standard TDHF, time-dependent single-particle wave functions of neutrons and protons are determined by their own self-consistent mean-field according to,

$$i\hbar \frac{\partial}{\partial t} \Phi_j^a(\vec{r}, t; \lambda) = h_a^\lambda \Phi_j^a(\vec{r}, t; \lambda). \quad (3)$$

Here $h_a^\lambda = p^2/2m_a + U_a(n_n^\lambda, n_p^\lambda)$ denotes the self-consistent mean-field Hamiltonian in the event, which depends on proton and neutron local densities $n_a^\lambda(r, t)$. We can express stochastic mean-field evolution in terms of single-particle density matrices of neutrons and protons as,

$$i\hbar \frac{\partial}{\partial t} \rho_a^\lambda(t) = [h_a^\lambda, \rho_a^\lambda(t)]. \quad (4)$$

In the stochastic mean-field approach an ensemble of single-particle density matrices is generated associated with different events. In this approach, we can calculate, not only the mean value of observables, also probability distribution of observables. Even if the magnitude of initial fluctuations is small, in particular in the vicinity of instabilities mean-field evolution can enhance the fluctuations, and hence events can substantially deviate from one another. By projecting on a collective path, it is demonstrated that the stochastic mean-field approach incorporates one-body dissipation and one-body fluctuation mechanisms in accordance with quantal dissipation-fluctuation relation [7].

In this work, we investigate the early growth of density fluctuations in spinodal region in charge asymmetric nuclear matter. For this purpose it is sufficient to consider the linear

response treatment of dynamical evolution [8]. The small amplitude fluctuations of the single-particle density matrix around an equilibrium state (ρ_n^0, ρ_p^0) are determined by the linearized TDHF equations. The linearized TDHF equations for fluctuations of neutron and proton density matrices, $\delta\rho_a^\lambda(t) = \rho_a^\lambda(t) - \rho_a^0$, are given by,

$$i\hbar \frac{\partial}{\partial t} \delta\rho_a^\lambda(t) = [h_a^0, \delta\rho_a^\lambda(t)] + [\delta U_a^\lambda(t), \rho_a^0]. \quad (5)$$

Since for infinite matter, the equilibrium state and the associated mean-field Hamiltonian h_a^0 are homogenous, it is suitable to analyze these equations in the plane wave representations,

$$i\hbar \frac{\partial}{\partial t} \langle \vec{p}_1 | \delta\rho_a(t) | \vec{p}_2 \rangle = [\varepsilon_a(\vec{p}_1) - \varepsilon_a(\vec{p}_2)] \langle \vec{p}_1 | \delta\rho_a(t) | \vec{p}_2 \rangle + [\rho_a(\vec{p}_1) - \rho_a(\vec{p}_2)] \langle \vec{p}_1 | \delta U_a(t) | \vec{p}_2 \rangle. \quad (6)$$

According to the basic assumption, matrix elements of the initial density matrix are Gaussian random numbers. In the plane wave representation the second moments of the initial correlations is given by,

$$\overline{\langle \vec{p}_1 | \delta\rho_a(0) | \vec{p}_2 \rangle \langle \vec{p}_2' | \delta\rho_b(0) | \vec{p}_1' \rangle} = \delta_{ab} (2\pi\hbar)^6 \delta(\vec{p}_1 - \vec{p}_1') \delta(\vec{p}_2 - \vec{p}_2') \frac{1}{2} [\rho_a(\vec{p}_1)(1 - \rho_a(\vec{p}_2)) + \rho_a(\vec{p}_2)(1 - \rho_a(\vec{p}_1))], \quad (7)$$

where the factor $(2\pi\hbar)^6$ arises from normalization of the plane waves.

III. GROWTH OF DENSITY FLUCTUATIONS

A. Spinodal Instabilities

In this section, we apply the stochastic mean-field approach in small amplitude limit to investigate spinodal instabilities in charge asymmetric nuclear matter [11]. We note that the following quantity

$$\delta\tilde{n}_a(\vec{k}, t) = 2 \int_{-\infty}^{\infty} \frac{d^3p}{(2\pi\hbar)^3} \langle \vec{p} + \hbar\vec{k}/2 | \delta\rho_a(t) | \vec{p} - \hbar\vec{k}/2 \rangle \quad (8)$$

defines the Fourier transform of the local density fluctuations of neutrons and protons. In this expression and in other formulas in this section, we omit the event label λ for clarity of notation. We can obtain solution of the linear response Eq. (6) by employing the standard method of one-sided Fourier transform in time,

$$\delta\tilde{n}_a(\vec{k}, \omega) = \int_0^{\infty} dt e^{i\omega t} \delta n_a(\vec{k}, t). \quad (9)$$

After transformation, we obtain a set of coupled algebraic equations for the Fourier transforms of fluctuating parts of local neutron and proton densities [12],

$$[1 + F_0^{nn} \chi_n(\vec{k}, \omega)] \delta \tilde{n}_n(\vec{k}, \omega) + F_0^{np} \chi_n(\vec{k}, \omega) \delta \tilde{n}_p(\vec{k}, \omega) = i A_n(\vec{k}, \omega) \quad (10)$$

and

$$[1 + F_0^{pp} \chi_p(\vec{k}, \omega)] \delta \tilde{n}_p(\vec{k}, \omega) + F_0^{pn} \chi_p(\vec{k}, \omega) \delta \tilde{n}_n(\vec{k}, \omega) = i A_p(\vec{k}, \omega). \quad (11)$$

In these expressions, derivative of the mean-field potential $U_a(n_n, n_p)$ evaluated at the equilibrium density $F_0^{ab} = (\partial U_b / \partial n_a)_0$ denotes the zero-order Landau parameters and $\chi_a(\vec{k}, \omega)$ is the Lindhard functions associated with neutron and proton distributions,

$$\chi_a(\vec{k}, \omega) = -2 \int_{-\infty}^{\infty} \frac{d^3 p}{(2\pi\hbar)^3} \frac{\rho_a(\vec{p} - \hbar\vec{k}/2) - \rho_a(\vec{p} + \hbar\vec{k}/2)}{\hbar\omega - \vec{p} \cdot \hbar\vec{k}/m}. \quad (12)$$

The source terms $A_a(\vec{k}, \omega)$ are determined by the initial conditions,

$$A_a(\vec{k}, \omega) = 2\hbar \int_{-\infty}^{\infty} \frac{d^3 p}{(2\pi\hbar)^3} \frac{\langle \vec{p} + \hbar\vec{k}/2 | \delta \rho_a(0) | \vec{p} - \hbar\vec{k}/2 \rangle}{\hbar\omega - \vec{p} \cdot \hbar\vec{k}/m}. \quad (13)$$

The solution of the coupled algebraic equations for Fourier transform of density fluctuations is given by,

$$\delta \tilde{n}_n(\vec{k}, \omega) = i \frac{[1 + F_0^{pp} \chi_p(\vec{k}, \omega)] A_n(\vec{k}, \omega) - F_0^{np} \chi_n(\vec{k}, \omega) A_p(\vec{k}, \omega)}{\varepsilon(\vec{k}, \omega)} \quad (14)$$

and

$$\delta \tilde{n}_p(\vec{k}, \omega) = i \frac{[1 + F_0^{nn} \chi_n(\vec{k}, \omega)] A_p(\vec{k}, \omega) - F_0^{pn} \chi_p(\vec{k}, \omega) A_n(\vec{k}, \omega)}{\varepsilon(\vec{k}, \omega)}, \quad (15)$$

where the quantity

$$\varepsilon(\vec{k}, \omega) = 1 + F_0^{nn} \chi_n(\vec{k}, \omega) + F_0^{pp} \chi_p(\vec{k}, \omega) + [F_0^{nn} F_0^{pp} - F_0^{np} F_0^{pn}] \chi_n(\vec{k}, \omega) \chi_p(\vec{k}, \omega) \quad (16)$$

denotes the susceptibility.

Time dependence of Fourier transform of density fluctuations $\delta \tilde{n}_a(\vec{k}, t)$ is determined by taking the inverse transformation of Eqs. (14) and (15) [13]. The inverse Fourier transformations in time can be calculated with the help of residue theorem, keeping only the growing and decaying collective poles we find,

$$\delta \tilde{n}_a(\vec{k}, t) = \delta n_a^+(\vec{k}) e^{+\Gamma_k t} + \delta n_a^-(\vec{k}) e^{-\Gamma_k t}, \quad (17)$$

where the initial amplitude of density fluctuations are given by

$$\delta n_n^\mp(\vec{k}) = - \left\{ \frac{[1 + F_0^{pp} \chi_p(\vec{k}, \omega)] A_n(\vec{k}, \omega) - F_0^{np} \chi_n(\vec{k}, \omega) A_p(\vec{k}, \omega)}{\partial \varepsilon(\vec{k}, \omega) / \partial \omega} \right\}_{\omega = \mp i \Gamma_k} \quad (18)$$

and

$$\delta n_p^\mp(\vec{k}) = - \left\{ \frac{[1 + F_0^{nn} \chi_n(\vec{k}, \omega)] A_p(\vec{k}, \omega) - F_0^{pn} \chi_p(\vec{k}, \omega) A_n(\vec{k}, \omega)}{\partial \varepsilon(\vec{k}, \omega) / \partial \omega} \right\}_{\omega = \mp i \Gamma_k} \quad (19)$$

Growth and decay rates $\omega = \mp i \Gamma_k$ are determined from the dispersion relation $\varepsilon(\vec{k}, \omega) = 0$, i.e. from the roots of susceptibility.

In numerical calculations we employ the same effective Skyrme potential as in reference [11],

$$U_a(n_n, n_p) = A \left(\frac{n}{n_0} \right) + B \left(\frac{n}{n_0} \right)^{\alpha+1} + C \left(\frac{n'}{n_0} \right) \tau_a + \frac{1}{2} \frac{dC}{dn} \frac{n'^2}{n_0} - D \Delta n + D' \Delta n' \tau_a \quad (20)$$

where $n = n_n + n_p$ and $n' = n_n - n_p$ are total and relative densities, and $\tau_a = +1$ for neutrons and $\tau_a = -1$ for protons. The parameters $A = -356.8 \text{ MeV}$, $B = +303.9 \text{ MeV}$, $\alpha = 1/6$ and $D = +130.0 \text{ MeV fm}^5$ are adjusted to reproduce the saturation properties of symmetric nuclear matter: The binding energy $\varepsilon_0 = 15.7 \text{ MeV/nucleon}$ and zero pressure at the saturation density $n_0 = 0.16 \text{ fm}^{-3}$, compressibility modulus $K = 201 \text{ MeV}$ and the surface energy coefficient in the Weizsacker mass formula $a_{surf} = 18.6 \text{ MeV}$ [14]. Magnitude of the parameter $D' = +34 \text{ MeV fm}^5$ is close to magnitude given by the SkM^* interaction [15]. The potential symmetry energy coefficient is $C(n) = C_1 - C_2(n/n_0)^\alpha$ with $C_1 = +124.9 \text{ MeV}$ and $C_2 = 93.5 \text{ MeV}$. These parameters for the symmetry energy coefficient in Weizsacker mass formula, at saturation density gives $a_{sym} = \varepsilon_F(n_0)/3 + C(n_0)/2 = 36.9/3 + 31.4/2 = 28.0 \text{ MeV}$.

As an example, Fig. 1(a) shows the growth rates of unstable modes as a function of wave number in the spinodal region corresponding to initial density $n = 0.2 n_0$ and $n = 0.4 n_0$ for initial asymmetry $I = 0.0$ at a temperature $T = 5 \text{ MeV}$. The initial charge asymmetry is defined according to $I = (n_n^0 - n_p^0)/(n_n^0 + n_p^0)$. In this figure and also in other figures, solid-lines and dashed-lines show quantal and semi-classical results, respectively. Since, at low densities, wave numbers of most unstable modes are comparable to Fermi momentum, long-wavelength expansion of the Linhard function is not valid, and hence there is important quantal effect in the dispersion relation. At the initial density $n = 0.2 n_0$ and the initial asymmetry $I = 0.0$, in the quantal calculations unstable modes are confined to a narrower

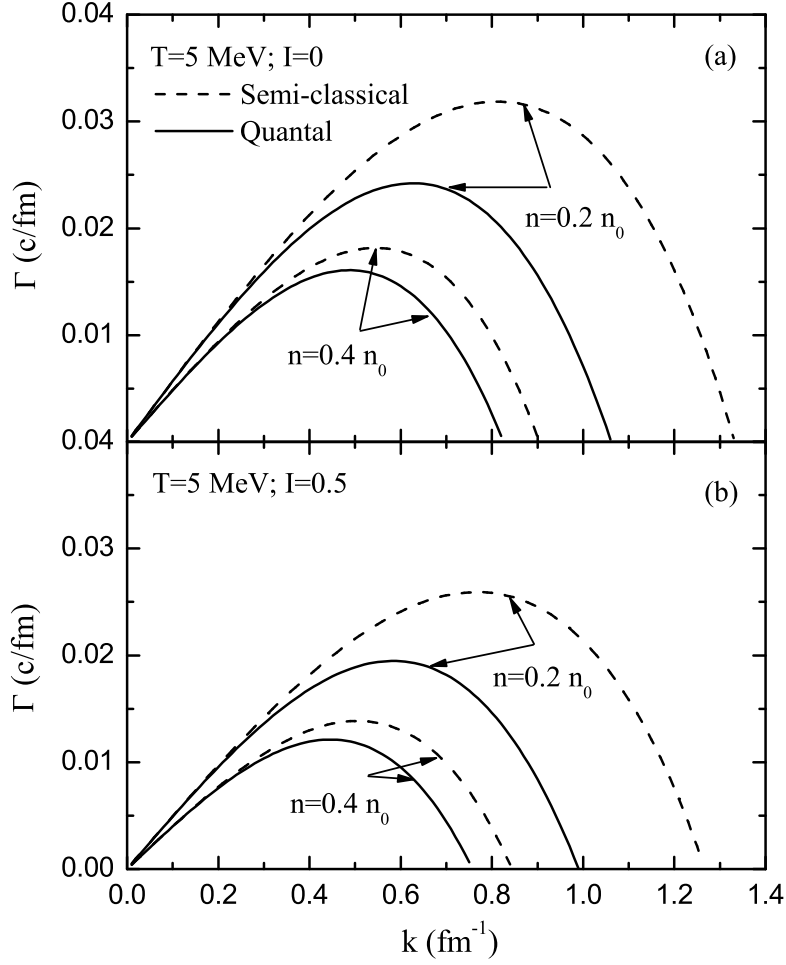


FIG. 1: Growth rates of unstable modes as a function of wave number in spinodal region corresponding initial densities and at a temperature $T = 5 \text{ MeV}$. (a) for initial asymmetry $I = 0.0$, (b) for initial asymmetry $I = 0.5$.

range centered around wavelengths $\lambda \approx 8 - 10 \text{ fm}$, as compared to a broader range centered around $\lambda \approx 7 \text{ fm}$ in the semi-classical calculations. Growth rates in semi-classical framework are determined by the roots of semi-classical susceptibility, which is defined as in Eq. (16) by taking the Lindhard functions $\chi_a(\vec{k}, \omega)$ in the long wavelength limit given by Eq. (28). As a result, in the quantal calculations, the source has a tendency to break up into larger fragments as compared to the semi-classical calculations. Also, due to quantum effects, the maximum of dispersion relation is reduced by about a factor $3/4$. Therefore, fluctuations

take more time to develop when quantum effects are introduced. At higher initial density $n = 0.4 n_0$, in both quantal and semi-classical calculations, dispersion relation is shifted towards longer wavelengths and it exhibits a similar trend as the one at the initial density $n = 0.2 n_0$. This quantal effect in dispersion relation of unstable modes was pointed out in the case of symmetric matter in a previous publication [16]. Charge asymmetric nuclear matter exhibits a similar behavior as seen from figure 1(b), which shows dispersion relation corresponding to initial densities $n = 0.2 n_0$ and $n = 0.4 n_0$ for initial charge asymmetry $I = 0.5$ at a temperature $T = 5 \text{ MeV}$. Figs. 2(a) and 2(b) shows the boundary of spinodal region in density-temperature plane corresponding to initial charge asymmetries $I = 0.0$ and $I = 0.5$ at a temperature $T = 5 \text{ MeV}$ for the unstable modes with wavelengths $\lambda = 9 \text{ fm}$ and $\lambda = 12 \text{ fm}$, respectively. It is seen that with increasing charge asymmetry, spinodal region shrinks to smaller size in both quantal and semi-classical calculations. Furthermore, unstable modes are quite suppressed by quantal effects as compared to the semi-classical results in both symmetric and asymmetric matter. Results of semi-classical calculation are in agreement with the result obtained in reference [11].

B. Growth of Density fluctuations

In this section, we calculate early growth of local density fluctuations in charge asymmetric nuclear matter. Spectral intensity of density correlation function $\tilde{\sigma}_{ab}(\vec{k}, t)$ is related to the second moment of Fourier transform of density fluctuations according to,

$$\tilde{\sigma}_{ab}(\vec{k}, t)(2\pi)^3\delta(\vec{k} - \vec{k}') = \overline{\delta\tilde{n}_a(\vec{k}, t)\delta\tilde{n}_b(-\vec{k}', t)}. \quad (21)$$

We calculate the spectral functions using the solution (17) and employing expression (7) for the initial correlations to find,

$$\tilde{\sigma}_{ab}(\vec{k}, t) = \frac{E_{ab}^+(\vec{k}, i\Gamma_k)}{|\partial\varepsilon(\vec{k}, \omega)/\partial\omega|_{\omega=i\Gamma_k}|^2}(e^{2\Gamma_k t} + e^{-2\Gamma_k t}) + \frac{2E_{ab}^-(\vec{k}, i\Gamma_k)}{|\partial\varepsilon(\vec{k}, \omega)/\partial\omega|_{\omega=i\Gamma_k}|^2} \quad (22)$$

where quantities $E_{ab}^\mp(\vec{k}, i\Gamma_k)$, $a, b = n, p$, are given by,

$$E_{nn}^\mp(\vec{k}, i\Gamma_k) = 4\hbar^2(1 + F_0^{pp}\chi_p)^2 I_n^\mp + 4\hbar^2(F_0^{np}\chi_n)^2 I_p^\mp, \quad (23)$$

$$E_{pp}^\mp(\vec{k}, i\Gamma_k) = 4\hbar^2(1 + F_0^{nn}\chi_n)^2 I_p^\mp + 4\hbar^2(F_0^{pn}\chi_p)^2 I_n^\mp \quad (24)$$

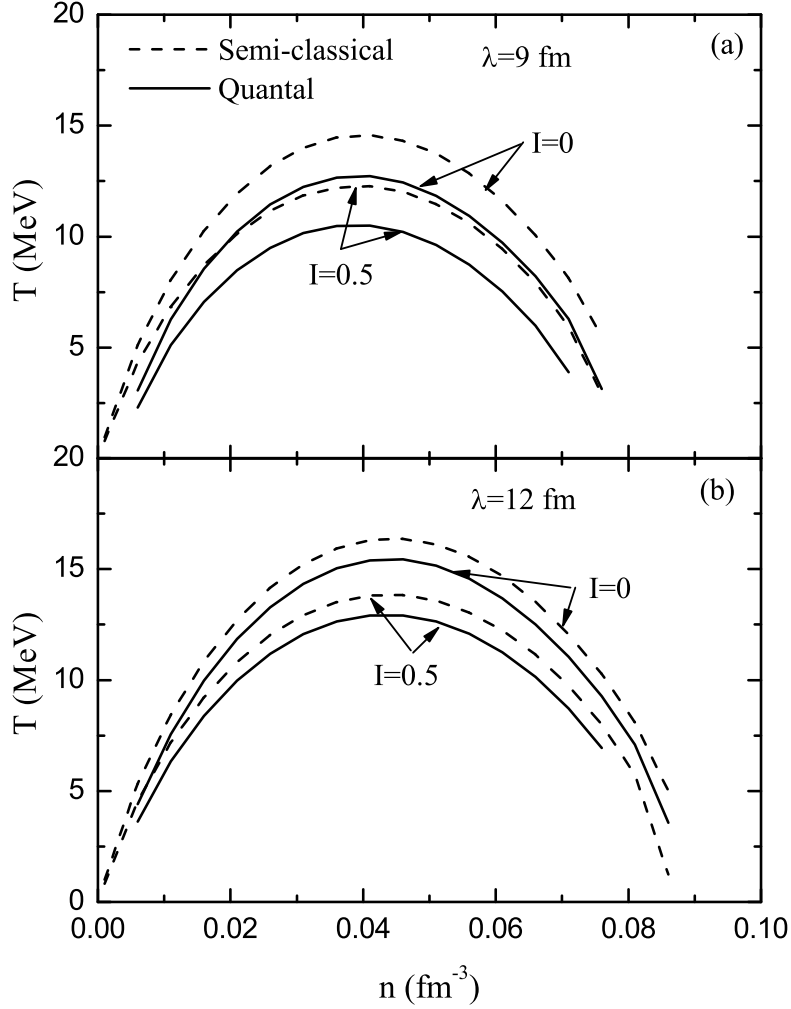


FIG. 2: Boundary of spinodal region in density-temperature plane corresponding to initial charge asymmetries $I = 0.0$ and $I = 0.5$ for the unstable mode: (a) with wavelength $\lambda = 9 \text{ fm}$, (b) with wavelength $\lambda = 12 \text{ fm}$.

and

$$E_{np}^{\mp}(\vec{k}, i\Gamma_k) = -4\hbar^2(1 + F_0^{pp}\chi_p)F_0^{pn}\chi_p I_n^{\mp} - 4\hbar^2(1 + F_0^{nn}\chi_n)F_0^{np}\chi_n I_p^{\mp} \quad (25)$$

with

$$I_a^{\mp} = \int \frac{d^3p}{(2\pi\hbar)^3} \frac{(\hbar\Gamma_k)^2 \mp (\vec{p} \cdot \hbar\vec{k}/m)^2}{[(\hbar\Gamma_k)^2 + (\vec{p} \cdot \hbar\vec{k}/m)^2]^2} \rho_a(\vec{p} + \hbar\vec{k}/2)[1 - \rho_a(\vec{p} - \hbar\vec{k}/2)]. \quad (26)$$

Semi-classical limit of these expressions are obtained by replacing the integrals I_a^\mp and $\chi_a(\vec{k}, \omega)$ with following expressions in the long wave-length limit,

$$I_a^\mp(sc) = \int \frac{d^3p}{(2\pi\hbar)^3} \frac{(\hbar\Gamma_k)^2 \mp (\vec{p} \cdot \hbar\vec{k}/m)^2}{[(\hbar\Gamma_k)^2 + (\vec{p} \cdot \hbar\vec{k}/m)^2]^2} \rho_a(\vec{p}) [1 - \rho_a(\vec{p})] \quad (27)$$

and

$$\chi_a^{sc}(\vec{k}, \omega) = -2 \int_{-\infty}^{\infty} \frac{d^3p}{(2\pi\hbar)^3} \frac{(\vec{p} \cdot \hbar\vec{k}/m)^2}{(\hbar\Gamma_k)^2 + (\vec{p} \cdot \hbar\vec{k}/m)^2} \frac{\partial}{\partial \varepsilon} \rho_a. \quad (28)$$

Figs. 3(a) and 3(b) shows spectral intensity $\tilde{\sigma}_{nn}(\vec{k}, t)$ of neutron-neutron density correlation function as function of wave number at times $t = 0$ and $t = 50 fm/c$ for density $n = 0.4 n_0$ and the initial charge asymmetry $I = 0.5$ at temperature $T = 1 MeV$ and $T = 5 MeV$, respectively.

As mentioned above, in all figures solid-lines and dashed-lines indicate quantal and semi-classical results, respectively. As seen, in particular at towards the high end of the wave number spectrum, considerable quantal effects are present at initial fluctuations. Quantum statistical effects in the initial fluctuations become even larger at smaller temperatures. In fact at zero temperature, since the quantities $I_a^\mp(sc)$ becomes zero, spectral functions vanish $\tilde{\sigma}_{ab}(\vec{k}, t) = 0$. However, in quantal calculations spectral functions remains finite even at zero temperature, reflecting quantum zero point fluctuations of the local density. Looking at the results at $t = 50 fm/c$, we observe that largest growth occurs over the range of wave numbers corresponding to the range of dominant unstable modes. At $T = 5 MeV$, magnitude of fluctuations is about the same in both quantal and semi-classical calculations. At the lower temperature $T = 1 MeV$, magnitude of fluctuations in the most unstable range is nearly doubled in quantal calculations as compared to semi-classical calculations. Fig. 3(c) shows spectral intensity $\tilde{\sigma}_{nn}(\vec{k}, t)$ as function of wave number at times $t = 0$ and $t = 50 fm/c$ at a lower density $n = 0.2 n_0$ for initial charge asymmetry $I = 0.5$ and temperature $T = 5 MeV$. At the lower density, growth rates of dominant modes in the semi-classical limit are considerably larger than those of quantal calculations. Consequently, the result of semi-classical calculations at time $t = 50 fm/c$ overshoots the result of quantal calculations over the range of dominant modes. Fig. 4 illustrates that the spectral intensity for symmetric matter has similar properties as for asymmetric matter with $I = 0.0$.

We note that quantal effects enter into the spectral density in two different ways: (i) quantal effects in growth rates of modes and (ii) quantum statistical effects on the initial

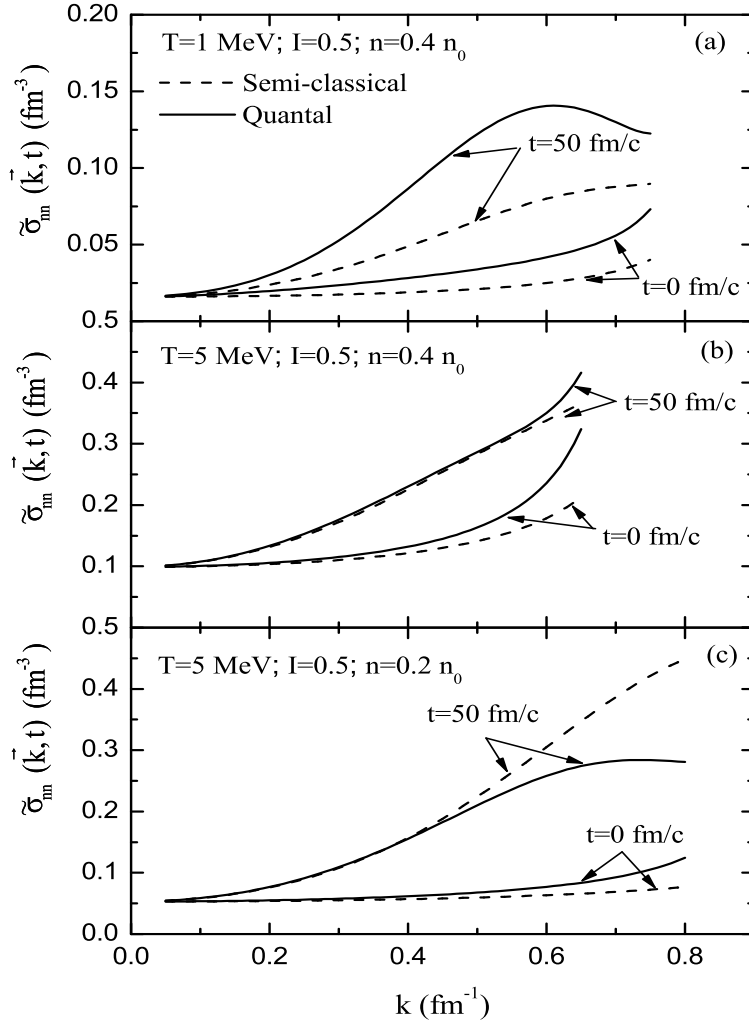


FIG. 3: Spectral intensity $\tilde{\sigma}_{nn}(\vec{k}, t)$ of neutron-neutron density correlation function as function of wave number k at times $t = 0$ and $t = 50 \text{ fm}/c$ for the initial charge asymmetry $I = 0.5$: (a) for density $n = 0.4 n_0$ at temperature $T = 1 \text{ MeV}$, (b) for density $n = 0.4 n_0$ at temperature $T = 5 \text{ MeV}$, (c) for density $n = 0.2 n_0$ at temperature $T = 5 \text{ MeV}$.

density fluctuations, which becomes increasingly more important at lower temperatures. We also note that in determining time evolution of $\delta\tilde{n}(\vec{k}, t)$ with the help of residue theorem, there are other contributions arising from non-collective poles of susceptibility $\varepsilon(\vec{k}, \omega)$ and from poles of $A_a(\vec{k}, \omega)$. These contributions, in particular towards short wavelengths, are important at the initial state, however they damp out in a short time interval [17]. Therefore the approximate expression (22) for the spectral intensity $\tilde{\sigma}(\vec{k}, t)$ of density fluctuations

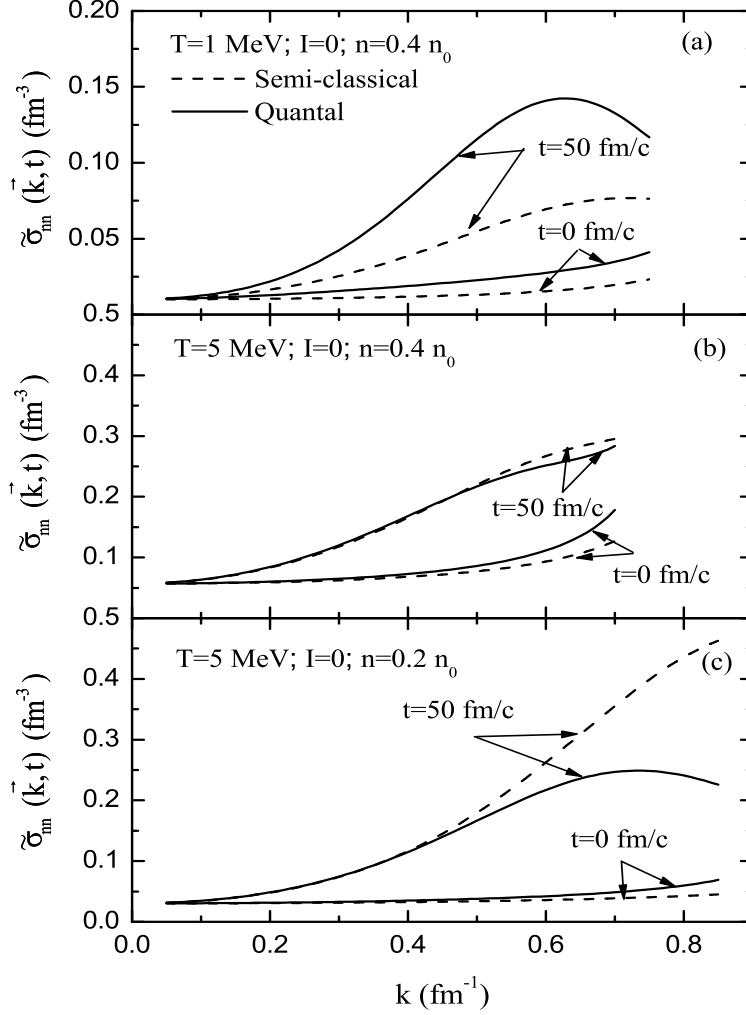


FIG. 4: Same as Fig. 3 but for asymmetry $I = 0.0$.

becomes more accurate for increasing time.

Local density fluctuations $\delta n_a(\vec{r}, t)$ are determined by the Fourier transform of $\delta \tilde{n}_a(\vec{k}, t)$. In terms of spectral intensity $\tilde{\sigma}_{ab}(\vec{k}, t)$, which is defined in Eq. (21), equal time density correlation function as a function of distance between two space locations is expressed as,

$$\sigma_{ab}(|\vec{r} - \vec{r}'|, t) = \overline{\delta n_a(\vec{r}, t) \delta n_b(\vec{r}', t)} = \int \frac{d^3 k}{(2\pi)^3} e^{i\vec{k} \cdot (\vec{r} - \vec{r}')} \tilde{\sigma}_{ab}(\vec{k}, t). \quad (29)$$

Total density correlation function is given by sum over neutrons and protons and cross-term, $\sigma(|\vec{r} - \vec{r}'|, t) = \sigma_{nn}(|\vec{r} - \vec{r}'|, t) + \sigma_{pp}(|\vec{r} - \vec{r}'|, t) + 2\sigma_{np}(|\vec{r} - \vec{r}'|, t)$. The behavior of density correlation function as a function of initial density and temperature carries valuable

information about the unstable dynamics of the matter in the spinodal region. As an example, Figs. 5(a) and 5(b) illustrate total density correlation function as a function of distance between two space points at times $t = 0$ and $t = 50 \text{ fm}/c$ at density $n = 0.4 n_0$ and the initial charge asymmetry $I = 0.5$ for temperatures $T = 1 \text{ MeV}$ and $T = 5 \text{ MeV}$, respectively. At temperature $T = 5 \text{ MeV}$, quantal effects are not important, and hence semi-classical calculations provide good approximation for density correlation function. However, at lower temperature $T = 1 \text{ MeV}$, semi-classical calculations severely underestimates peak value of density correlation function. Fig. 5(c) shows density correlation function at times $t = 0$ and $t = 50 \text{ fm}/c$ at a lower density $n = 0.2 n_0$ for initial charge asymmetry $I = 0.5$ and a temperature $T = 5 \text{ MeV}$. On the other hand, at lower density, semi-classical approximation overestimates the peak value of the correlation function. As indicated above, this is due to the fact that growth rates of dominant modes in semi-classical limit are considerably larger than those obtained in quantal calculations. For asymmetry $I = 0.0$, as seen from Fig. 6, behavior of density correlation function is similar to the charge asymmetric case. Complementary to the dispersion relation, correlation length of density fluctuations provides an additional measure for the average size of primary fragmentation pattern. We can estimate the correlation length of density fluctuations as the width of correlation function at half maximum. Correlation length depends on density, and to some extent, depends on temperature as well. From these figures, we can estimate that the correlation length of density fluctuations is about 3.5 fm at density $n = 0.4 n_0$, and about 3.0 fm at density $n = 0.2 n_0$.

During spinodal decomposition, initial charge asymmetry shifts towards symmetry in liquid phase while gas phase moves toward further asymmetry. As a result, produced fragments are more symmetric than the charge asymmetry of the source. This interesting fact is experimentally observed and it may provide a useful guidance to gain information about symmetry energy in low density nuclear matter. For each event, we can define perturbation charge asymmetry during early evolution of density fluctuations as,

$$I_{pt} = \frac{\delta n_n(\vec{r}, t) - \delta n_p(\vec{r}, t)}{\delta n_n(\vec{r}, t) + \delta n_p(\vec{r}, t)} = \frac{[\delta n_n(\vec{r}, t)]^2 - [\delta n_p(\vec{r}, t)]^2}{[\delta n_n(\vec{r}, t) + \delta n_p(\vec{r}, t)]^2}. \quad (30)$$

We are interested in the ensemble average value of this quantity, which can approximately be evaluated according to

$$\bar{I}_{pt} \approx \frac{\sigma_{nn}(t) - \sigma_{pp}(t)}{\sigma_{nn}(t) + 2\sigma_{np}(t) + \sigma_{pp}(t)}. \quad (31)$$

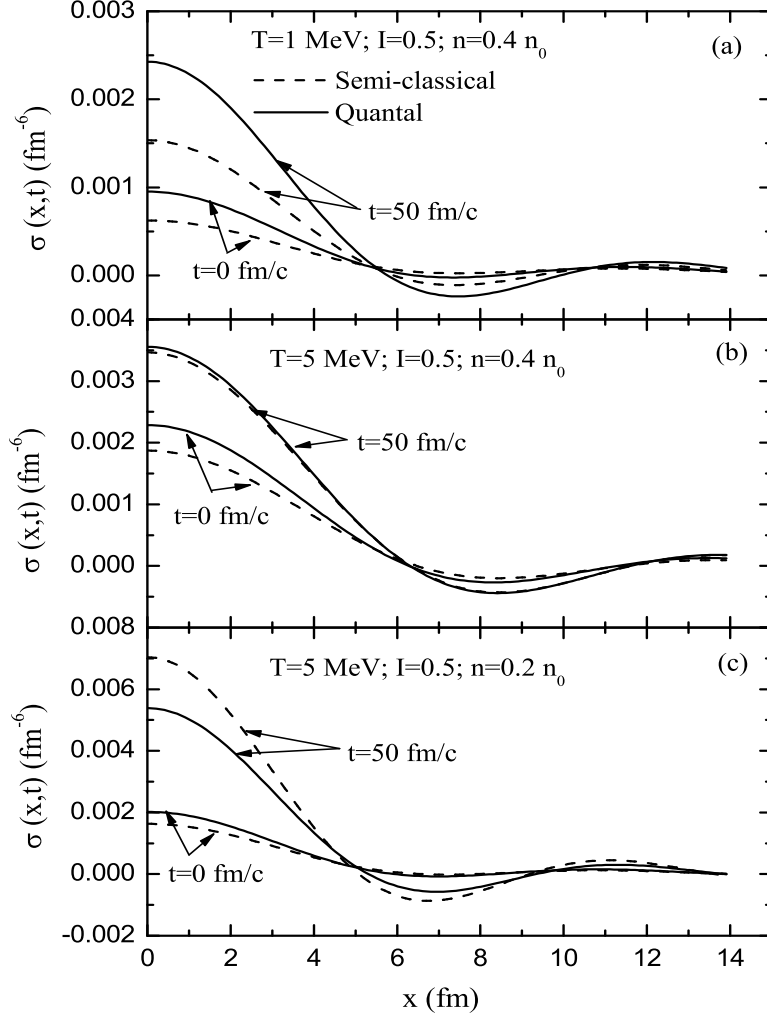


FIG. 5: Density correlation function $\sigma(x,t)$ as a function of distance $x = |\vec{r} - \vec{r}'|$ between two space points at times $t = 0$ and $t = 50 \text{ fm}/c$ and the initial charge asymmetry $I = 0.5$: (a) for density $n = 0.4 n_0$ at temperature $T = 1 \text{ MeV}$, (b) for density $n = 0.4 n_0$ at temperature $T = 5 \text{ MeV}$, (c) for density $n = 0.2 n_0$ at temperature $T = 5 \text{ MeV}$.

where $\sigma_{ab}(t) = \sigma_{ab}(|\vec{r} - \vec{r}'| = 0, t)$. The average value of the perturbation asymmetry is nearly independent of time. As an example, Fig. 7 shows this quantity as function of initial asymmetry at temperature $T = 5 \text{ MeV}$ for densities $n = 0.2 n_0$ and $n = 0.4 n_0$. As a result of the driving force of symmetry energy, perturbation asymmetry drifts towards symmetry. At this temperature quantal effects do not play an important role and these calculations are

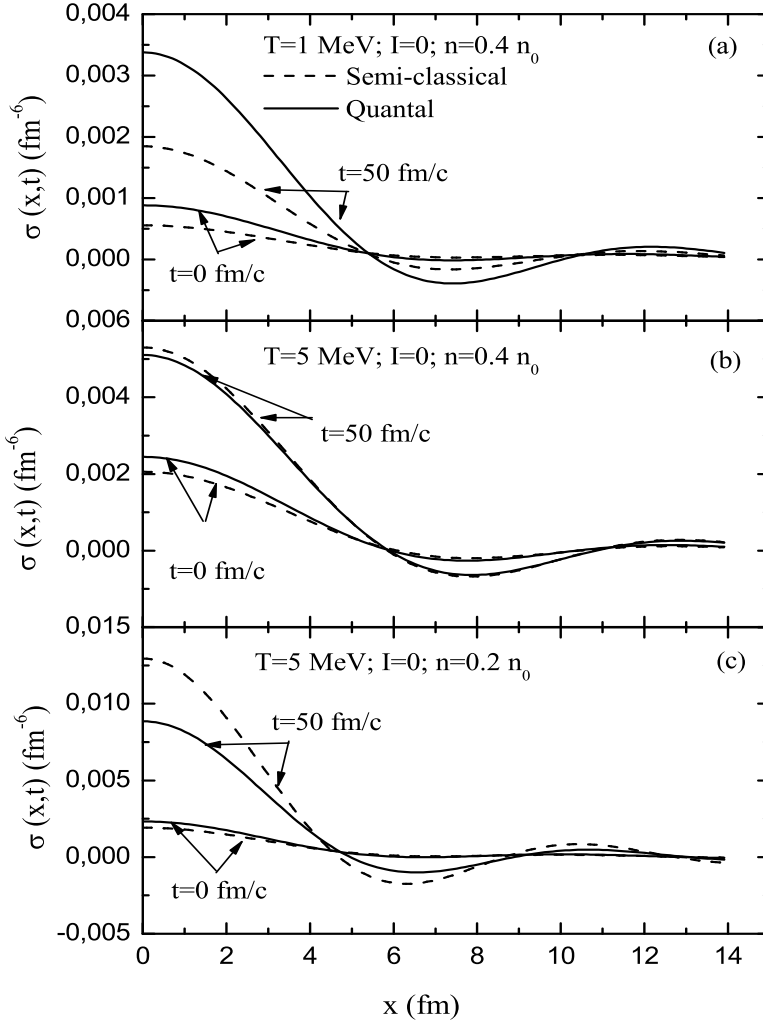


FIG. 6: Same as Fig. 5 but for asymmetry $I = 0.0$.

consistent with results of ref. [11].

IV. CONCLUSIONS

Recently proposed stochastic mean-field theory incorporates both one-body dissipation and fluctuation mechanisms in a manner consistent with quantal fluctuation-dissipation theorem of non-equilibrium statistical mechanics. Therefore, this approach provides a powerful tool for microscopic description of low energy nuclear processes in which two-body dissipation and fluctuation mechanisms do not play important role. The low energy processes

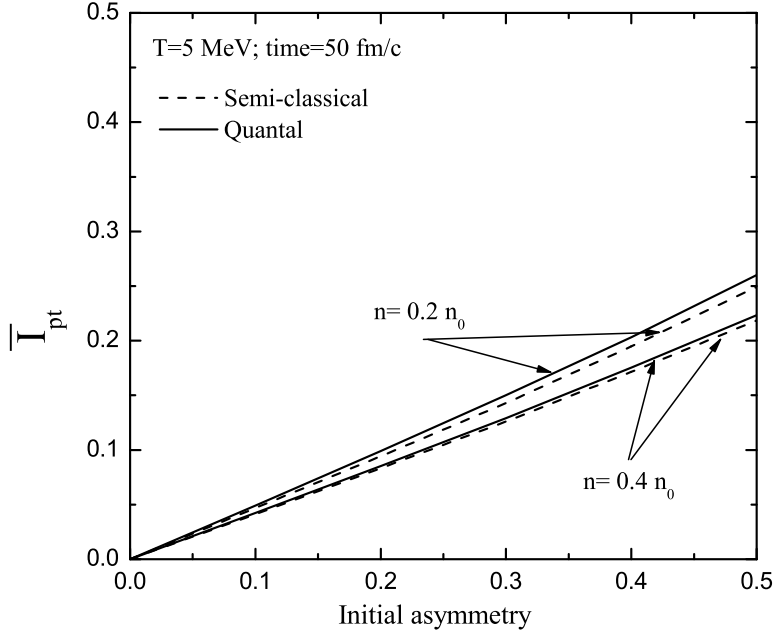


FIG. 7: Perturbation asymmetry as function of initial asymmetry at temperature $T = 5 \text{ MeV}$ for densities $n = 0.2 n_0$ and $n = 0.4 n_0$.

include induced fission, heavy-ion fusion near barrier energies, spinodal decomposition of nuclear matter and nuclear multi-fragmentations. In this work we investigate quantal effects on spinodal instabilities and early growth of density fluctuations in charge asymmetric nuclear matter. For this purpose it is sufficient to consider the linear response treatment of the stochastic mean-field approach. Retaining only growing and decaying collective modes, it is possible to calculate time evolution of spectral intensity of density correlation function and the density correlation function itself including quantum statistical effects. Growth rates of unstable collective modes are determined from a quantal dispersion relation, i.e. from the roots of susceptibility. Due to quantal effects, growth rates of unstable modes, in particular with wave numbers larger than the Fermi momentum, are strongly suppressed. As a result, dominant collective modes are shifted to longer wavelengths than those obtained in the semi-classical description with the same effective interaction, in both symmetric and asymmetric matter. The size of spinodal zone associated with these modes is reduced by the quantal effects. In calculation of density correlation function, quantal effects enter into

the description through the growth rates of the modes and through the initial density fluctuations. Quantum statistical influence on density correlation functions grows larger at lower temperatures and also at lower densities. Quantal effects appear to be important for a quantitative description of spinodal instabilities and growth of density fluctuations in an expanding nuclear system. Stochastic mean-field approach incorporates both one-body dissipation and fluctuations mechanisms in a manner consistent with dissipation-fluctuation theorem. Therefore, it will be very interesting to investigate spinodal decomposition of an expanding nuclear system in this framework. We also note that numerical effort in simulation of stochastic mean-field approach is not so much greater than the effort required in solving ordinary three dimensional time dependent Hartree-Fock equations.

Acknowledgments

One of us (S.A.) gratefully acknowledges TUBITAK for a partial support and the Physics Department of Middle East Technical University for warm hospitality extended to him during his visit. This work is supported in part by the US DOE grant No. DE-FG05-89ER40530 and in part by the TUBITAK grant No. 107T691.

-
- [1] P. Ring and P. Schuck, "The Nuclear Many-Body Problem", Springer, New York, (1980).
 - [2] K.T.D. Davis, K. R. S. Devi, S. E. Koonin and M. Strayer, "Treatise in Heavy-Ion Science", ed. D. A. Bromley, Nuclear Science V-4, Plenum, New York, (1984).
 - [3] W. Cassing, U. Mosel, Prog. Part. Nucl. Phys. **25** (1990) 1.
 - [4] S. Ayik and C. Gregoire, Phys. Lett. **B 212** (1988) 269 ; Nucl. Phys. **A 513** (1990) 187.
 - [5] J. Randrup and B. Remaud, Nucl. Phys. **A 514** (1990) 339.
 - [6] Y. Abe, S. Ayik, P.-G. Reinhard, and E. Suraud, Phys. Rep. **275** (1996) 49 .
 - [7] S. Ayik, Phys. Lett. **B 658** (2008) 174 .
 - [8] Ph. Chomaz, M. Colonna and J. Randrup, Phys. Rep. **389** (2004) 263 .
 - [9] S. Ayik, M. Colonna and Ph. Chomaz, Phys. Lett. **353** (1995) 417 .
 - [10] M. Colonna, Ph. Chomaz and S. Ayik, Phys. Rev. Lett. **88** (2002) 122701 .
 - [11] V. Baran, M. Colonna, M. Di Toro and A. B. Larionov, Nucl. Phys. **A 632** (1998) 287 .

- [12] H. Heiselberg, C. J. Pethick and D. G. Ravenhall, Phys. Rev. Lett. **61** (1988) 818.
- [13] E. M. Lifshitz and L. P. Pitaevskii, "Physical Kinetics", Pergamon, (1981).
- [14] G. Baym, H. A. Bethe and C. J. Pethick, Nucl. Phys. **A 175** (1971) 225.
- [15] H. Krivine, J. Treiner and O. Bohigas, Nucl. Phys. **A 336** (1990) 155 .
- [16] S. Ayik, M. Colonna and Ph. Chomaz, Phys. Lett. **B 353** (1995) 417 .
- [17] P. Bozek, Phys. Lett. **B 383** (1996) 121.